



INL Collaboration in Neutron Capture Therapy Research with the University of Missouri

David W. Nigg, Nuclear Science and Engineering Division, INL

John D. Brockman, University of Missouri Research Reactor

M. Frederick Hawthorne, University of Missouri

Stuart Slattery, University of Wisconsin

Woo Y. Yoon, Nuclear Science and Engineering Division, INL

Washington DC ANS Local Section Meeting

October 13, 2009



Acknowledgements

- *This work is sponsored by the University of Missouri through the MU International Institute for Nano and Molecular Medicine and by the INL Education Programs Office through the Faculty-Staff Exchange, Division Initiative, and Student Support programs*
- *The University of Missouri Research Reactor organization provided essential logistics, engineering and machine shop support*
- *Some in-kind contributions of special materials needed for this project were made by the US Department of Energy through the Idaho National Laboratory*
- *Dr. Robert Brugger, former MURR Director and former INL Nuclear Technology Division Director, provided essential advice and suggestions in the early part of this project. His contributions to the overall fields of Neutron Capture Therapy and Reactor Physics are gratefully acknowledged*



Overview

- *NCT history and research progress*
- *Description of the INL/MU collaboration and the new MU radiobiological research facility*
- *Computed and measured neutronic performance of the new single-crystal filtered neutron beam at MU*
- *Future plans -- Path forward*



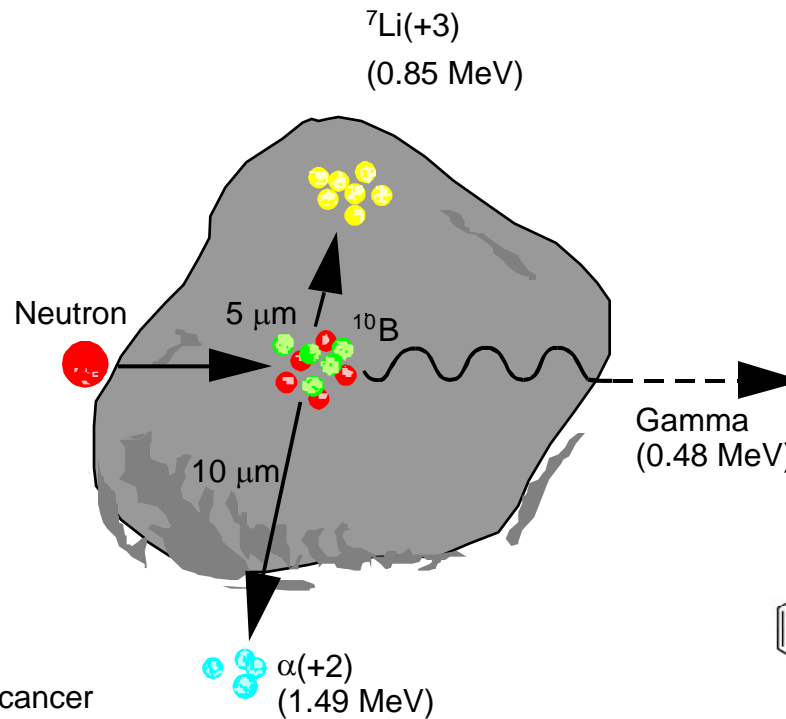
Boron Neutron Capture Therapy

In situ activation reaction, $^{10}\text{B}(n, \alpha) ^7\text{Li}$; releases ionizing energy within volume of single cancer cell:

Targets of traditional and current interest:

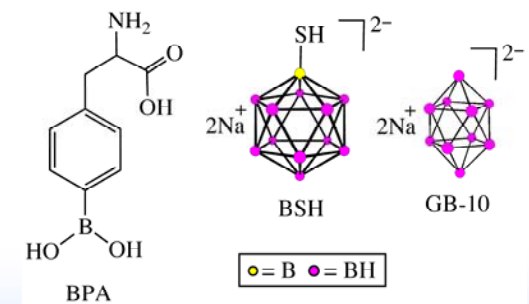
- **High-grade Glioma**
- **Primary and Metastatic Melanoma**
- **Head and Neck Tumors**
- **Metastatic Liver Tumors**

Average cancer cell is about 10 μm in diameter.



Current FDA approved boron delivery agents:

- **BSH: Borocaptate Sodium**
- **BPA: Boronated Phenylalanine**
- **GB-10: $\text{Na}_2\text{B}_{10}\text{H}_{10}$**



MT=107 : (z,a) Cross section for B10 from ENDFB 6.8 from Local



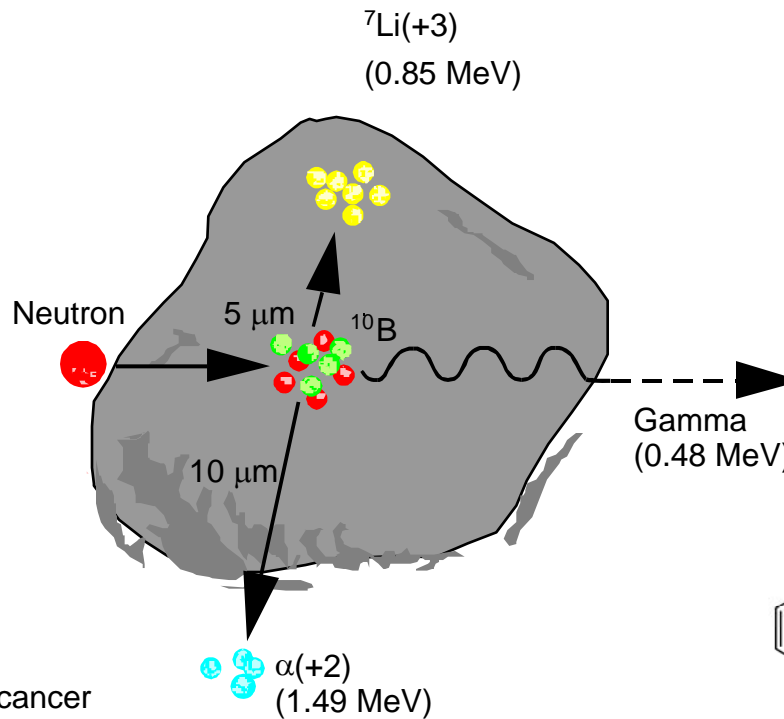
Boron Neutron Capture Therapy

In situ activation reaction, $^{10}\text{B}(n, \alpha) ^7\text{Li}$; releases ionizing energy within volume of single cancer cell:

Targets of traditional and current interest:

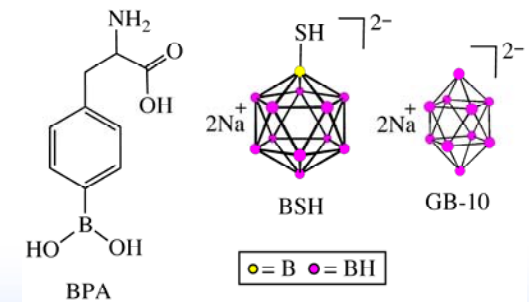
- **High-grade Glioma**
- **Primary and Metastatic Melanoma**
- **Head and Neck Tumors**
- **Metastatic Liver Tumors**

Average cancer cell is about 10 μm in diameter.



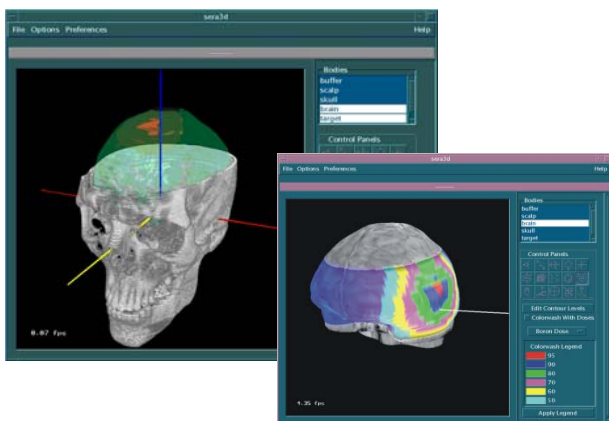
Current FDA approved boron delivery agents:

- **BSH: Borocaptate Sodium**
- **BPA: Boronated Phenylalanine**
- **GB-10: $\text{Na}_2\text{B}_{10}\text{H}_{10}$**

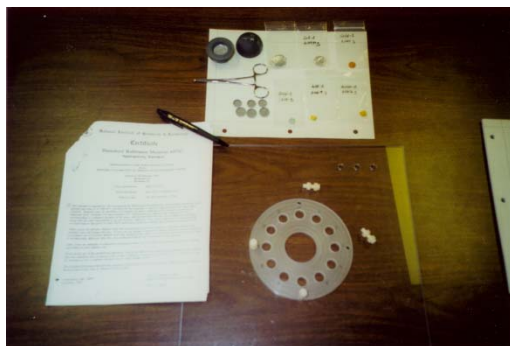


INL Advanced Radiotherapy Program

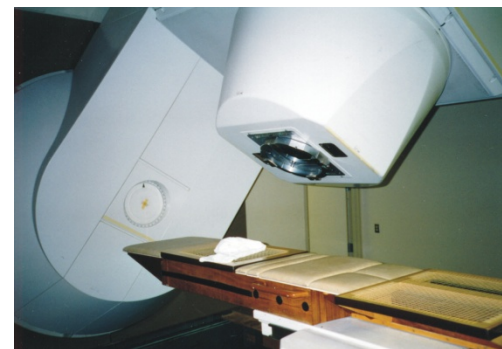
Key Historical Components



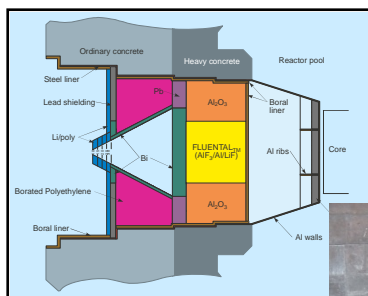
Development of advanced software for computational medical dosimetry



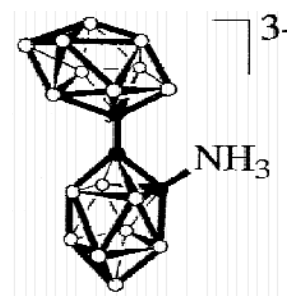
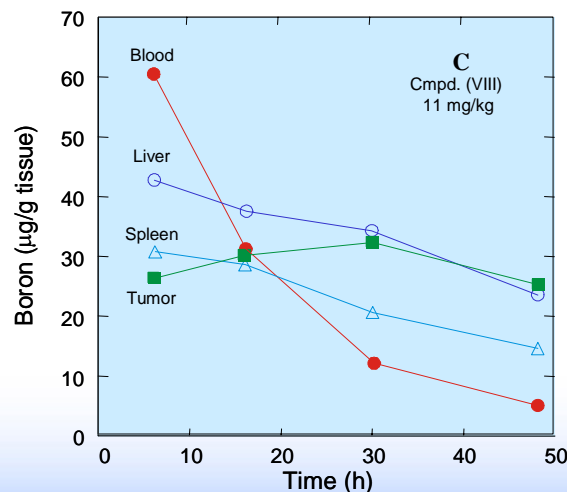
Development of advanced methods for medical neutron dosimetry



Research collaboration with University of Washington for development of neutron capture enhanced fast-neutron therapy



Design, construction, and dosimetry support for epithermal neutron beam user facility for neutron capture therapy research at Washington State University



Synthesis, biochemical analysis and preclinical testing of advanced boron agents for neutron capture therapy

M. F. Hawthorne, et al., *Proc. Natl. Acad. Sci. USA*
Vol 91, pp. 3029-3033, April 1994

BNCT is progressing ---- But only slowly in the USA

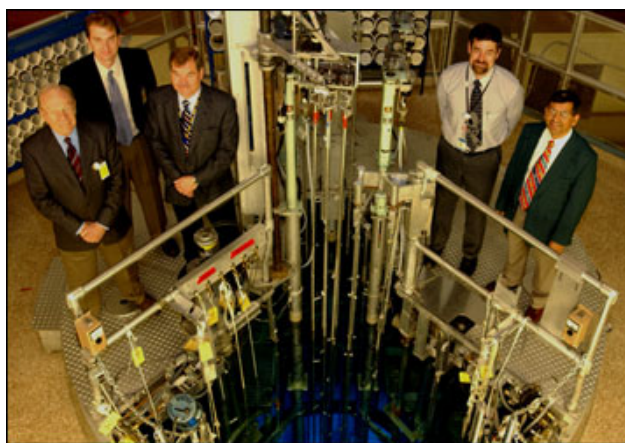
- ***“Modern” epithermal trials at MIT and BNL 1994-1999 (BPA) sponsored by US Department of Energy. INL provided key modeling and simulation technologies, experimental beam dosimetry, and analytical chemistry for the BNL trials and has collaborated with others worldwide.***
- ***Epithermal trials at the JRC Petten Facility initiated in 1995 (BSH).***
- ***20-40 Patients per year in Finland (BPA). Trials continuing since 1999.***
- ***Japanese clinical applications begun in 1968 continue (BPA/BSH).***
- ***Human studies initiated in Argentina in 2005 (BPA)***
- ***Neutron sources have reached high levels of development, and dosimetry is continuously improving. The next advances are likely to require improved boron delivery agents.***

The situation in the US has been uncertain since 2006. But the US community is still quietly participating

- ***University of Missouri-INL Collaboration – Improved Boron Agent Development – Dosimetry modeling, simulation and validation. New neutron source construction.***
- ***CNEA-INL Collaboration – Combined agent studies (BPA-GB10)***



University of Missouri International Institute of Nano and Molecular Medicine



Hawthorne, far left, and fellow MU nanotechnology leader Kattesh Katti, PhD, far right, collaborate with colleagues at MU's Nuclear Research Reactor.



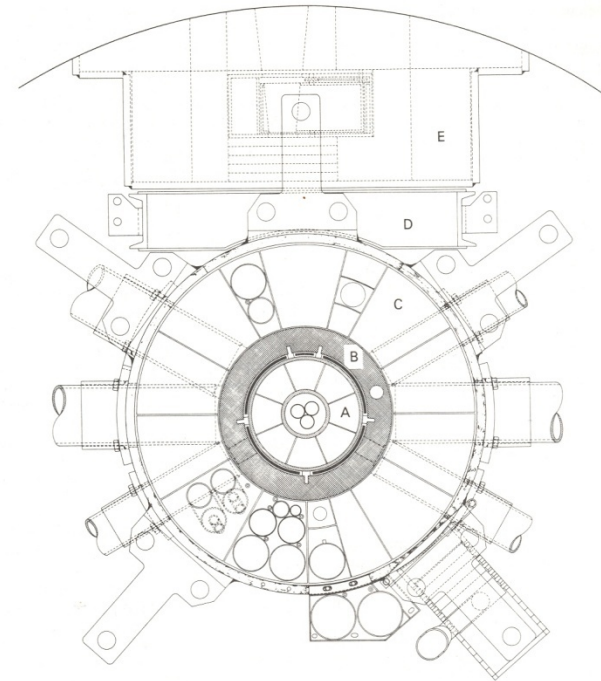
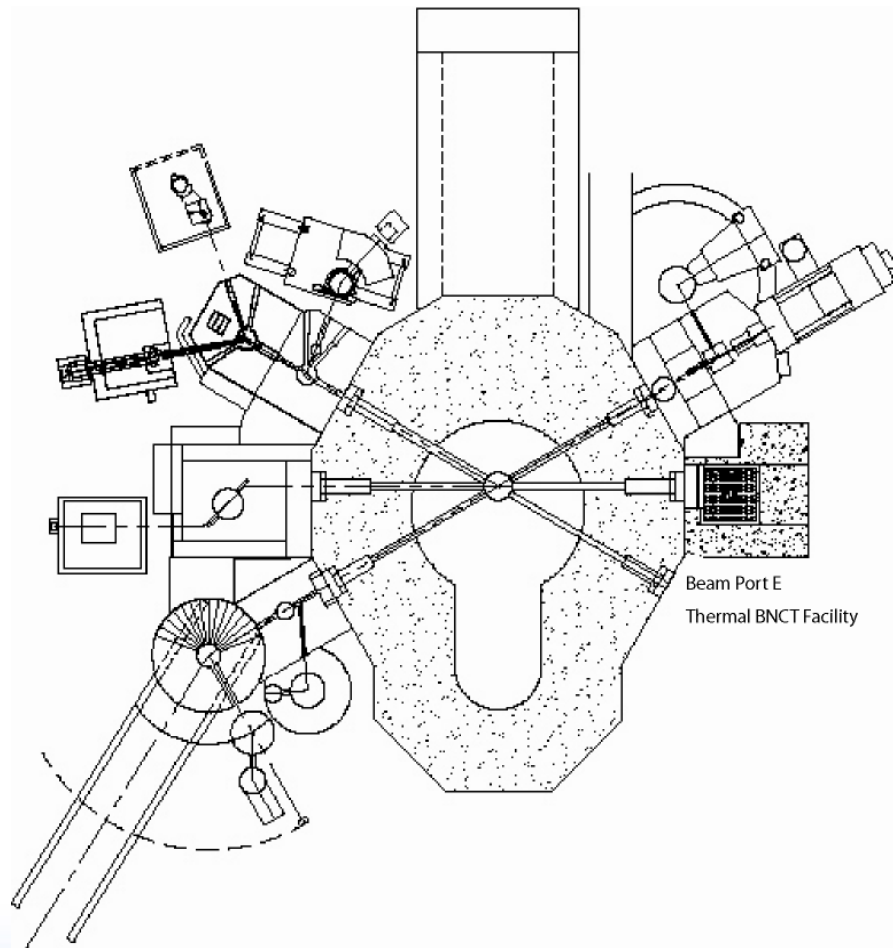
Frederick Hawthorne, PhD, describes boron's similarity to carbon during a lecture at MU. His discoveries involving boron have contributed greatly to a new field of science with particularly important applications for medicine.

Hawthorne at helm of nanomedicine institute

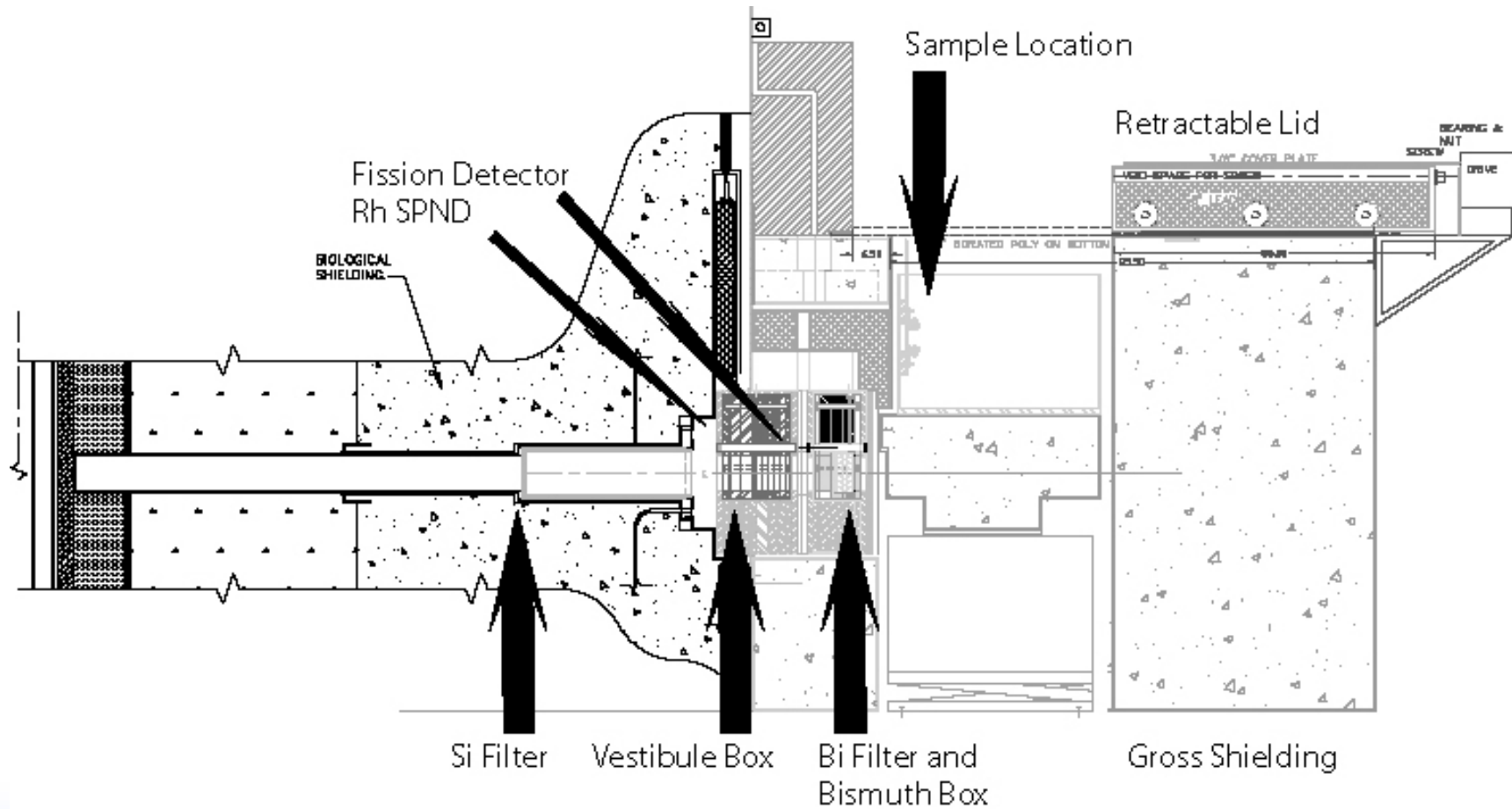
MU has big plans for tiny particles



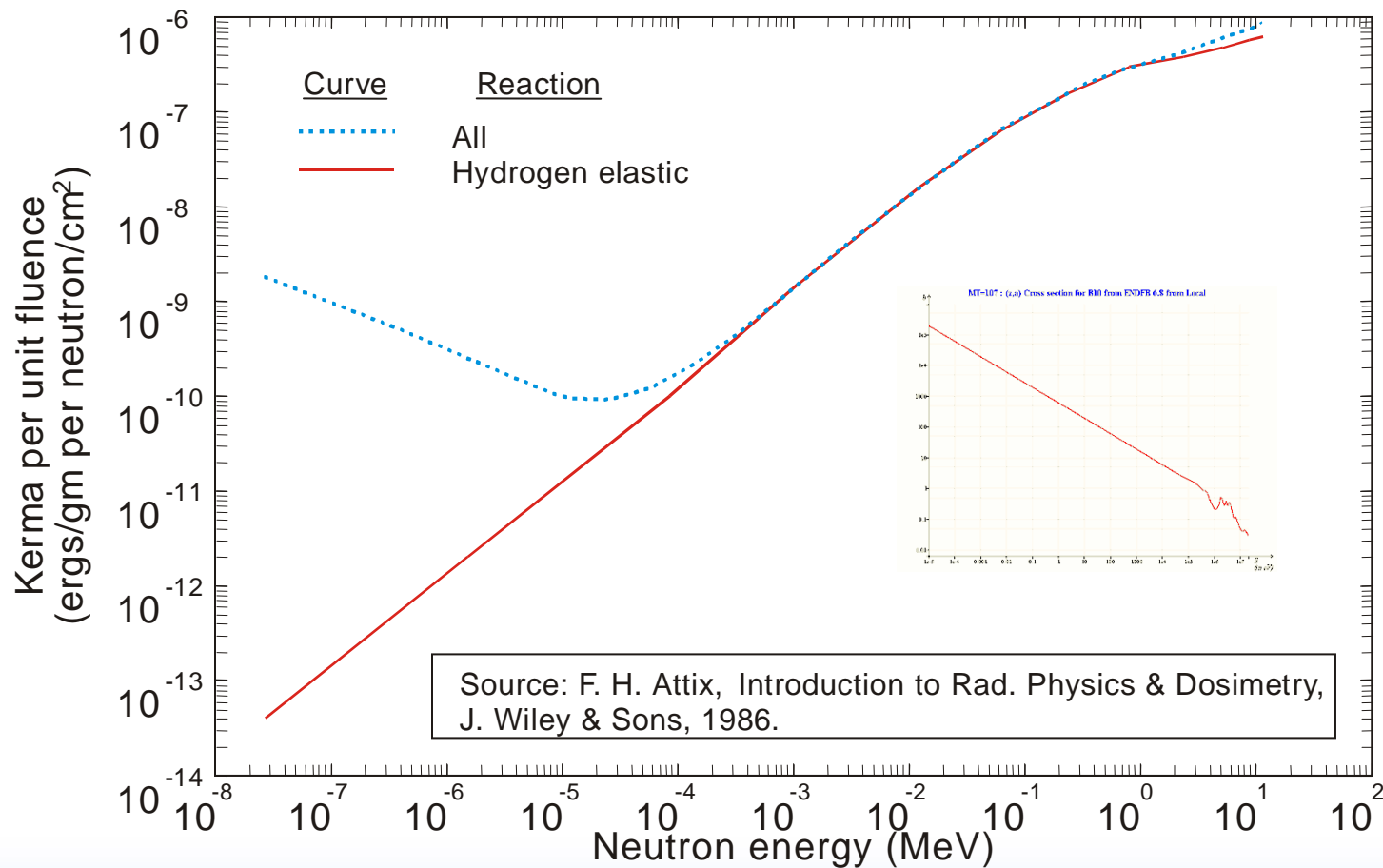
University of Missouri Research Reactor



MURR Beamline E with NCT Modifications



Contributions to Background Neutron Kerma in Tissue



Neutron Filtering Crystals

Silicon

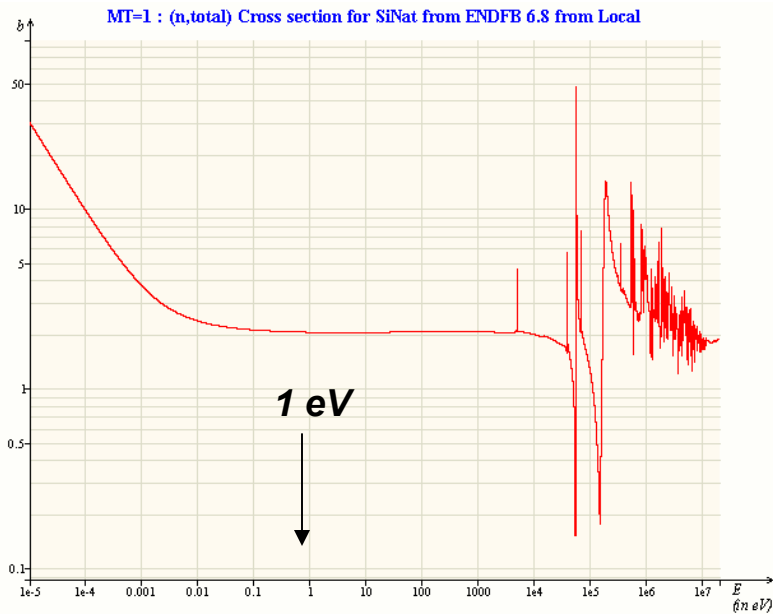


Bismuth

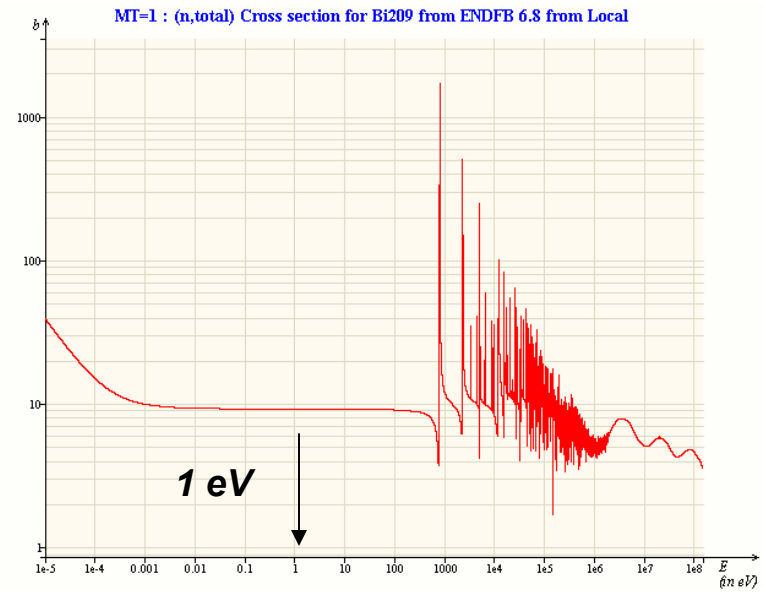


Silicon and Bismuth Total Cross Sections (Amorphous)

Si (Natural)



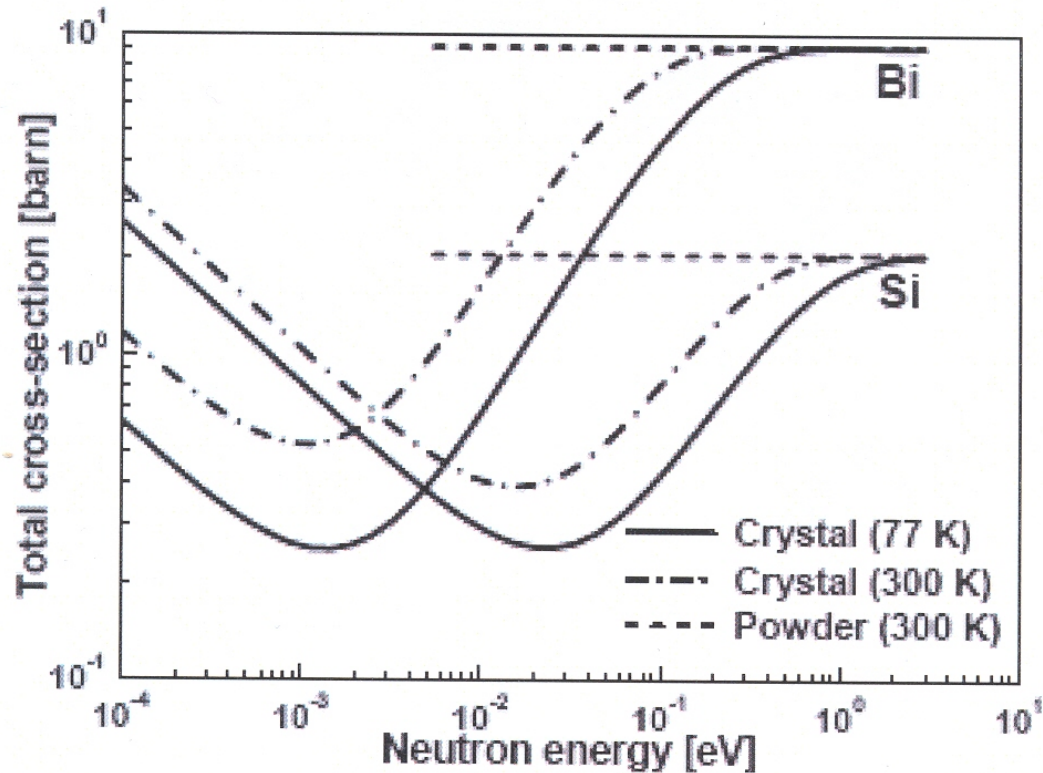
²⁰⁹Bi



Source: OECD-NEA (Janis)



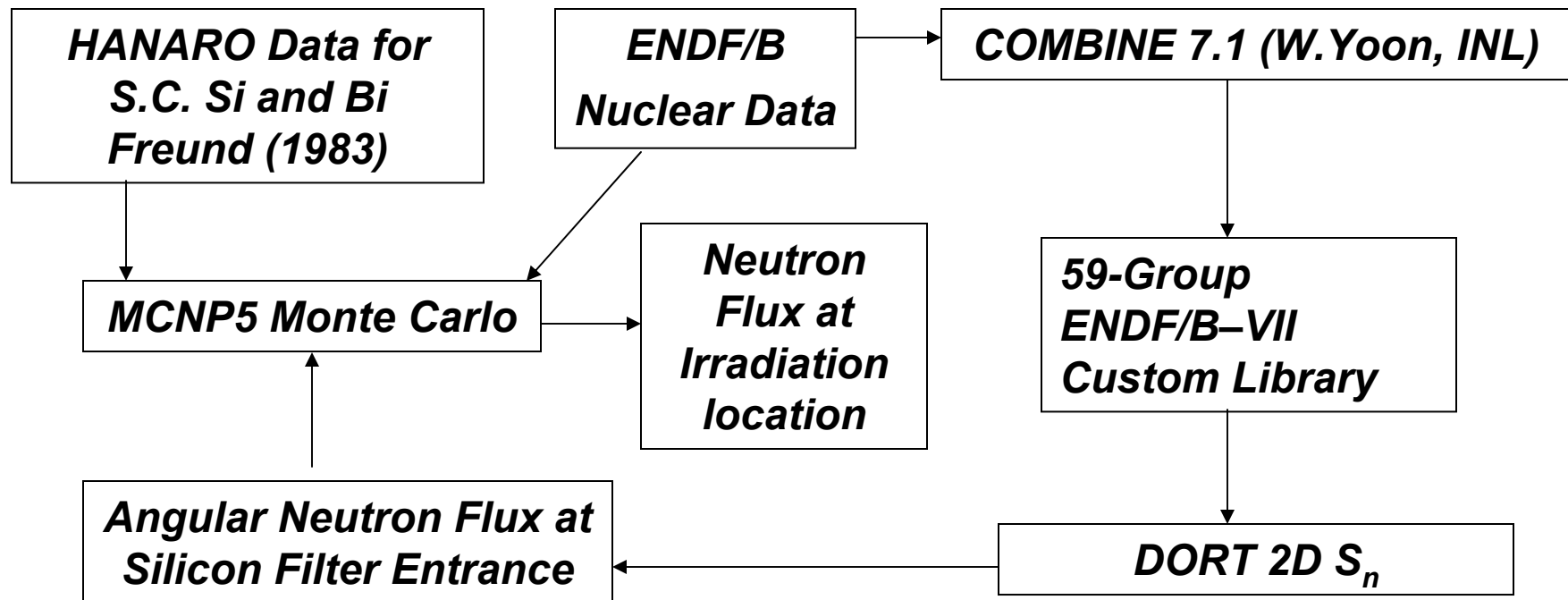
Thermal Cross Sections for Silicon and Bismuth



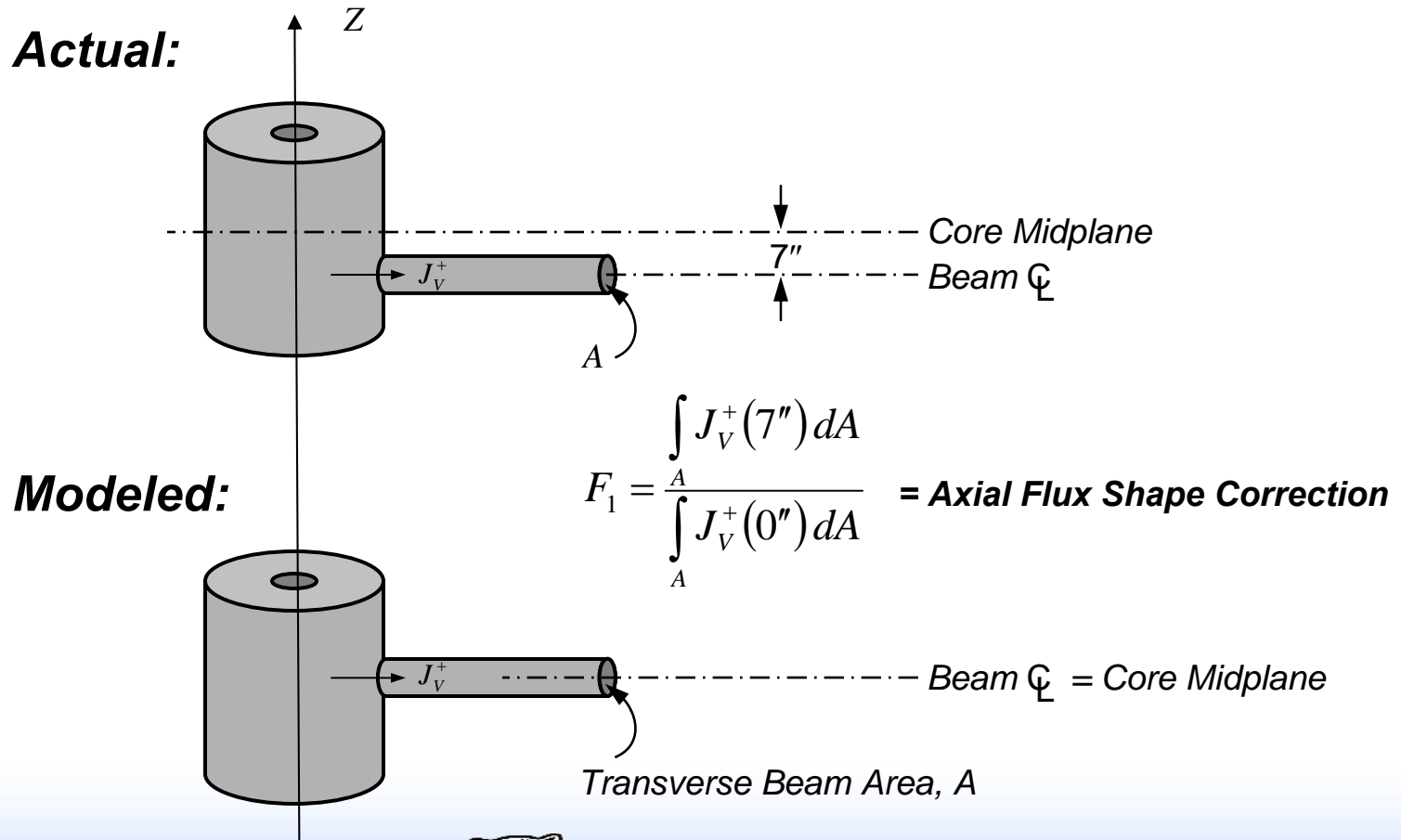
Source: Kim et al. Phys. Med. Bio (2007)

Upgrade to Computational Modeling

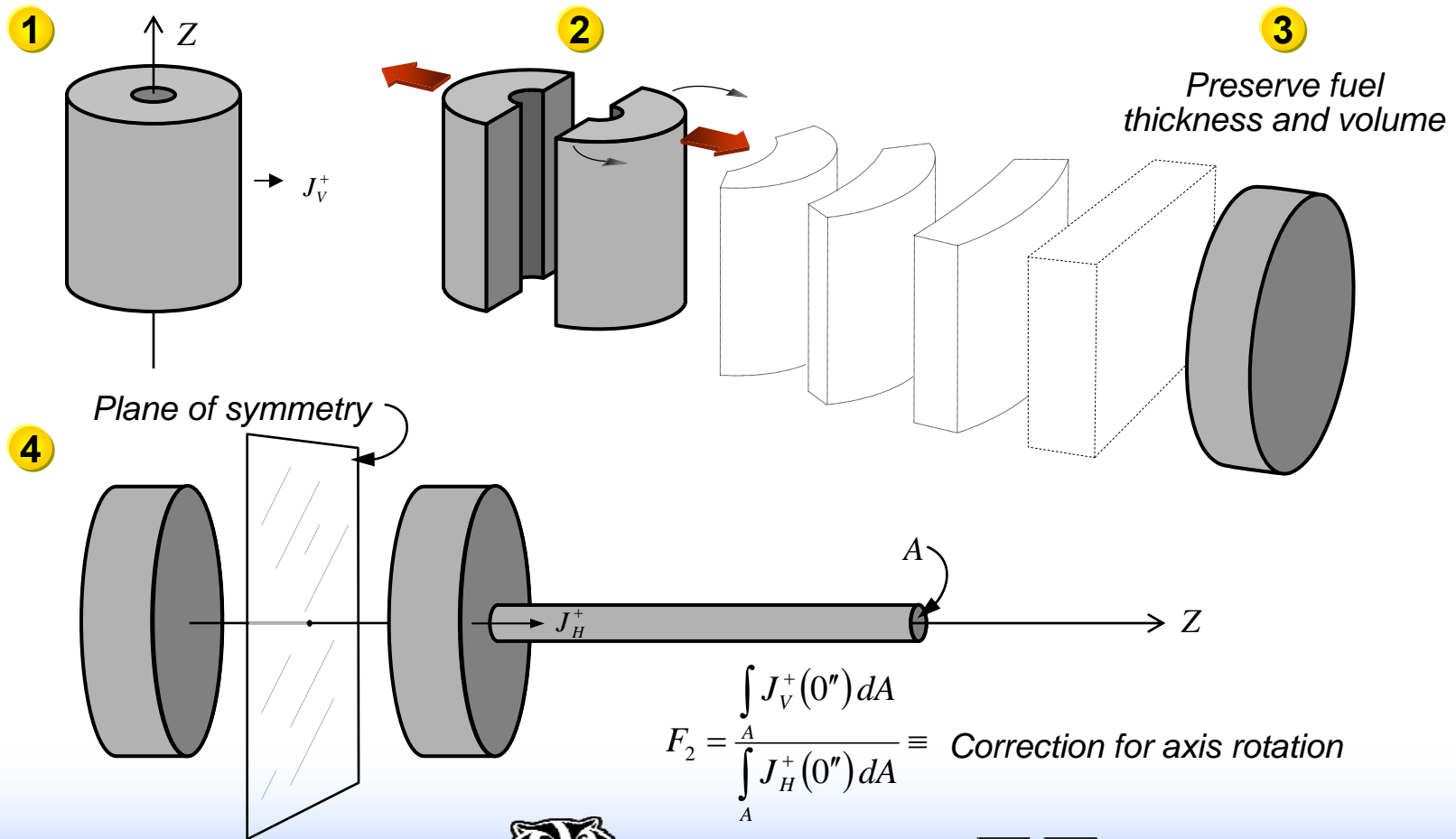
Summer 2009, Stuart Slattery, University of Wisconsin



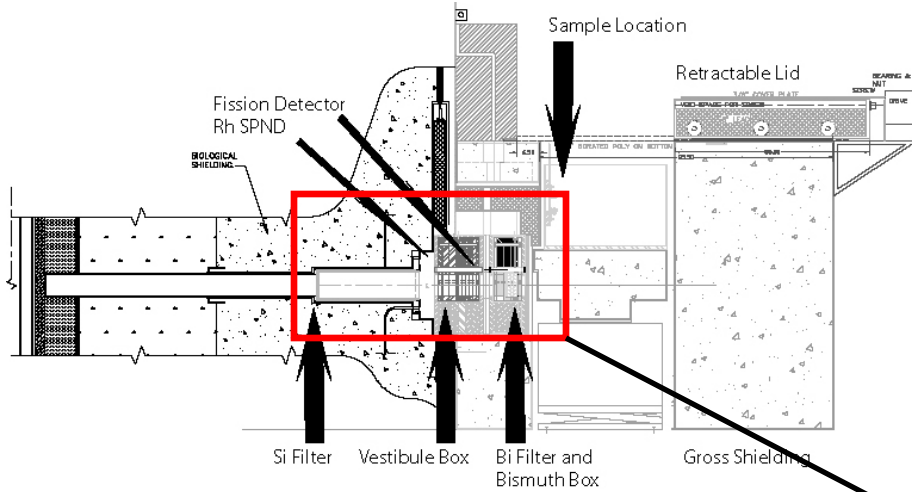
Geometric Projections for Discrete-Ordinates Modeling (Vertical Beamline Translation)



Geometric Projections for Discrete-Ordinates Modeling (Core Axis Rotation)

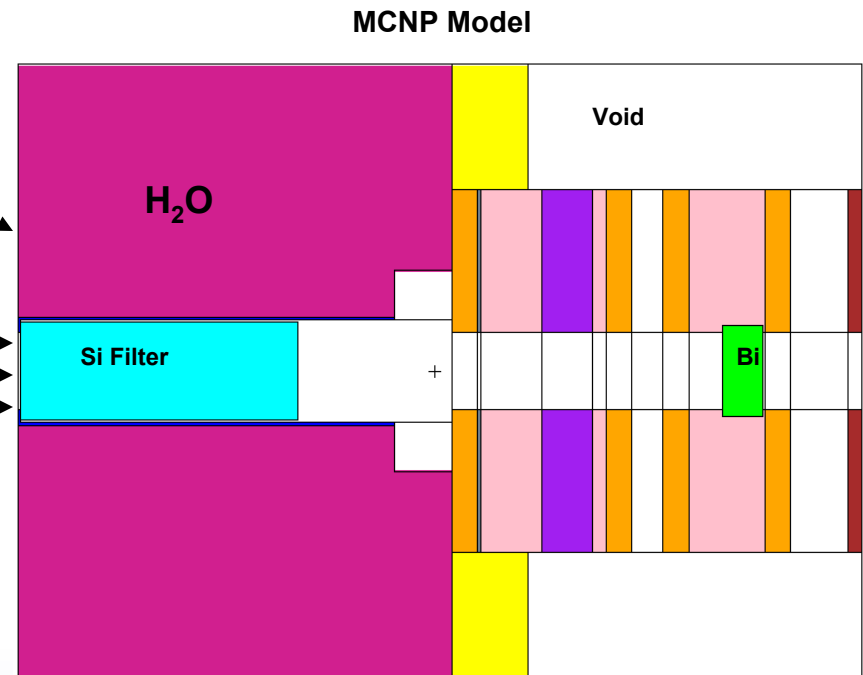


MURR Beamline Model



- The DORT beamline model contains the entire beamline from the reactor to the irradiation location modeled in cylindrical geometry.
- A plane source from the reactor model is saved and then loaded into the MCNP beamline filter submodel.

Source spectrum from DORT beamline calculation



Final Beamstop and Irradiation Facility Shielding under Construction by MURR Staff



Activation Interactions Used for Initial MURR Beamline E Neutron Spectrum Measurements

Neutron Interaction	Energy Range of Primary Response	Activation Gamma Energy (keV)	Nominal Foil Mass (mg)
$^{197}\text{Au} (n, \gamma)$ Bare Foil $^{55}\text{Mn} (n, \gamma)$ Bare Foil	Thermal Thermal	411 847	60 50
$^{115}\text{In} (n, \gamma)$ Cd Cover	1 eV Resonance	1293, 1097, and 416	25
$^{197}\text{Au} (n, \gamma)$ Cd Cover	5 eV Resonance	411	60
$^{186}\text{W} (n, \gamma)$ Cd Cover	18 eV Resonance	686	60
$^{55}\text{Mn} (n, \gamma)$ Cd Cover	340 eV Resonance	847	50
$^{63}\text{Cu} (n, \gamma)$ Cd Cover	1 keV Resonance	511 (Positron)	140
$^{115}\text{In} (n, n')$ Boron Sphere	300 keV Threshold	336	4000

Beam Aperture Plate and Activation Foil Holder

**INL
Foil
Holder**

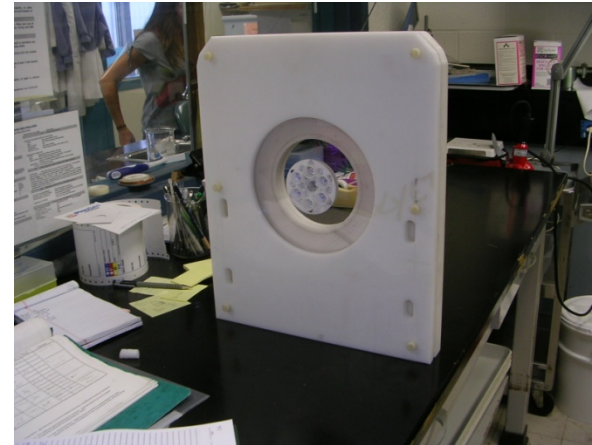


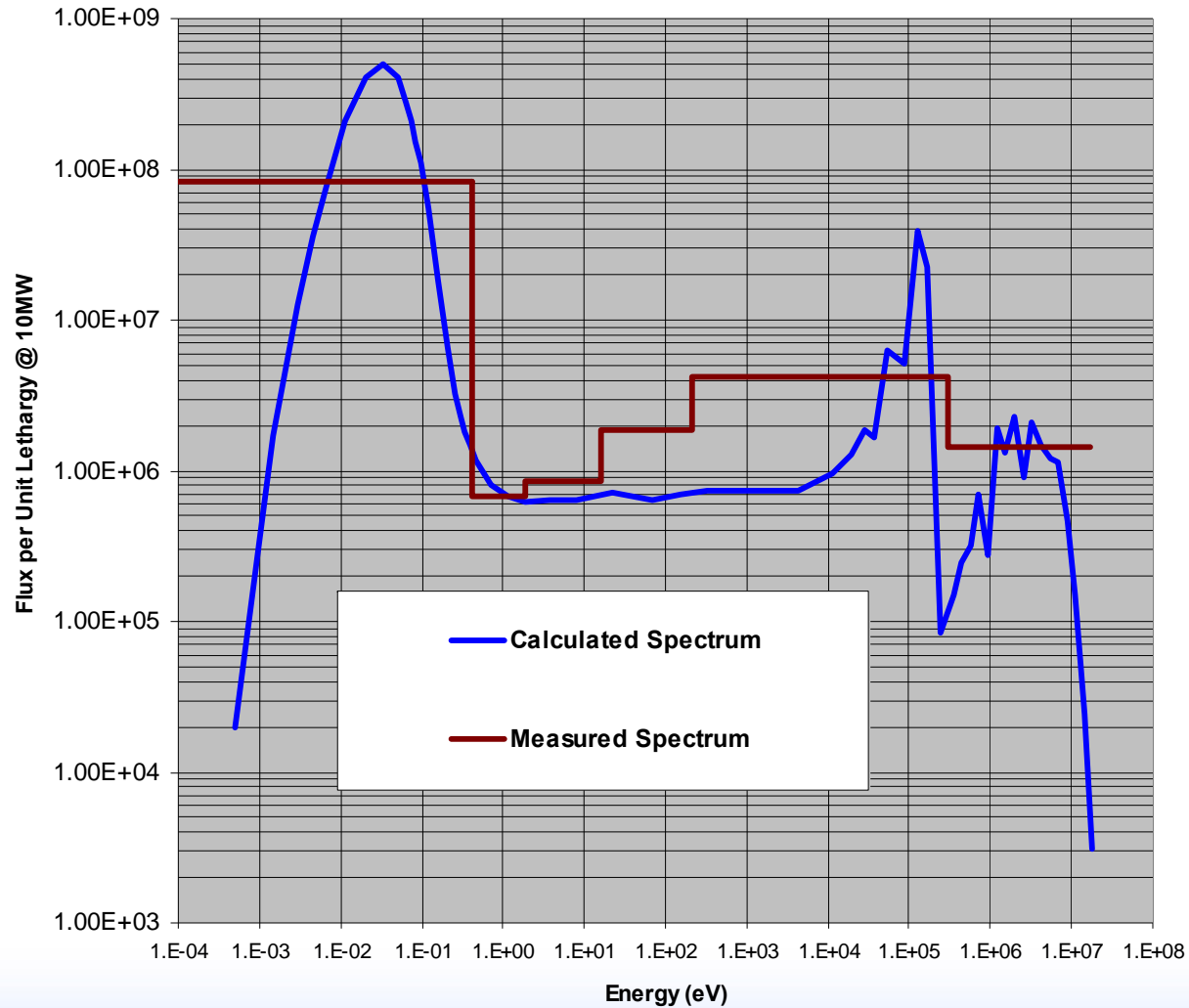
**Plate
assembly
fabricated
by MURR
machine
shop staff**

**Insertion
of
Aperture
Plate**

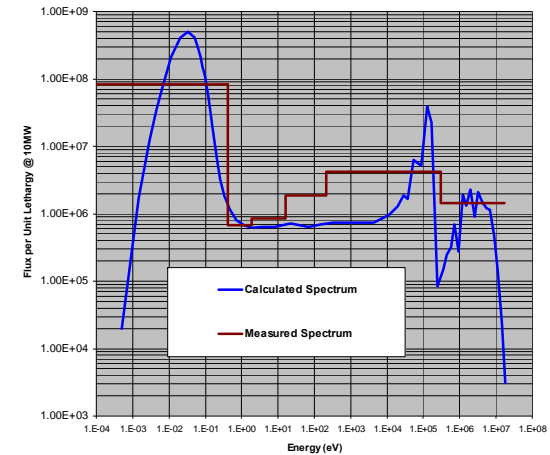


**Shield
Closure**

Single Crystal Filtered Beamline Model Comparison



Integral Parameters



Single Crystal Filtered Beam Thermal Flux				
Data Source	Flux@10MW		% Difference	Uncertainty (1σ)
Laboratory Measurement	8.80E+08	n/cm ² s	-----	6%
BUGLE-80 DORT Model	9.62E+08	n/cm ² s	9.30%	10%
COMBINE 7.1 DORT/MCNP Model	9.20E+08	n/cm ² s	4.55%	4.06%



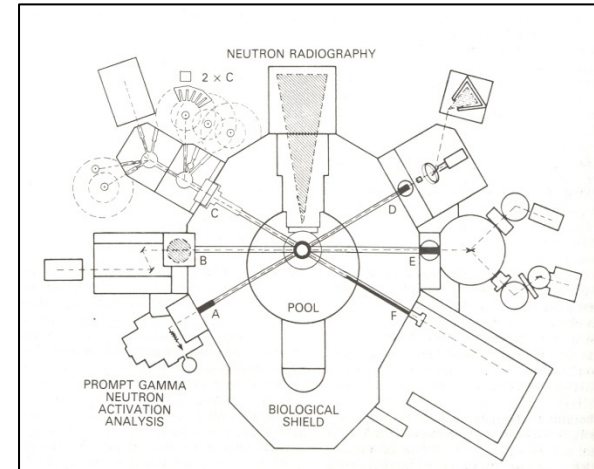
Foil Reaction Rates – Measured vs Direct Least-Square Fit

<u>Shield</u>	<u>Reaction</u>	<u>A-Priori</u>	<u>Measured</u>	<u>L.S. Fit</u>	<u>Difference (%)</u>
Boron	In-115 (n,n')	5.63E-19	1.240E-18	1.210E-18	-2.42
Boron	In-115 (n,n')	5.63E-19	1.150E-18	1.210E-18	5.22
Boron	In-115 (n,n')	5.63E-19	1.260E-18	1.210E-18	-3.97
Boron	In-115 (n,n')	5.63E-19	1.200E-18	1.210E-18	0.83
Cd	Cu-63 (n,g)	2.56E-18	6.930E-18	6.048E-18	-12.73
Cd	Cu-63 (n,g)	2.56E-18	6.770E-18	6.048E-18	-10.67
Cd	Mn-55 (n,g)	6.97E-18	1.430E-17	1.579E-17	10.40
Cd	Mn-55 (n,g)	6.97E-18	1.420E-17	1.579E-17	11.18
Cd	W-186 (n,g)	1.61E-16	4.050E-16	3.900E-16	-3.72
Cd	W-186 (n,g)	1.61E-16	3.940E-16	3.900E-16	-1.03
Cd	W-186 (n,g)	1.61E-16	4.020E-16	3.900E-16	-3.00
Cd	W-186 (n,g)	1.61E-16	3.700E-16	3.900E-16	5.39
Cd	Au-197 (n,g)	4.19E-16	6.540E-16	6.304E-16	-3.62
Cd	Au-197 (n,g)	4.19E-16	6.410E-16	6.304E-16	-1.66
Cd	Au-197 (n,g)	4.19E-16	6.200E-16	6.304E-16	1.67
Cd	Au-197 (n,g)	4.19E-16	6.140E-16	6.304E-16	2.66
Cd	In-115 (n,g)	8.41E-16	1.130E-15	1.141E-15	0.96
Cd	In-115 (n,g)	8.41E-16	1.170E-15	1.141E-15	-2.49
Cd	In-115 (n,g)	8.41E-16	1.120E-15	1.141E-15	1.87
Cd	In-115 (n,g)	8.41E-16	1.130E-15	1.141E-15	0.96
Cd	In-115 (n,g)	8.41E-16	1.170E-15	1.141E-15	-2.49
Cd	In-115 (n,g)	8.41E-16	1.140E-15	1.141E-15	0.08
Bare	Au-197 (n,g)	9.09E-14	8.290E-14	8.377E-14	1.05
Bare	Au-197 (n,g)	9.09E-14	7.910E-14	8.377E-14	5.91
Bare	Au-197 (n,g)	9.09E-14	8.920E-14	8.377E-14	-6.09
Bare	Au-197 (n,g)	9.09E-14	8.370E-14	8.377E-14	0.08
Bare	Mn-55 (n,g)	1.23E-14	1.100E-14	1.131E-14	2.81
Bare	Mn-55 (n,g)	1.23E-14	1.130E-14	1.131E-14	0.08
Bare	Mn-55 (n,g)	1.23E-14	1.190E-14	1.131E-14	-4.97
Bare	Mn-55 (n,g)	1.23E-14	1.130E-14	1.131E-14	0.08



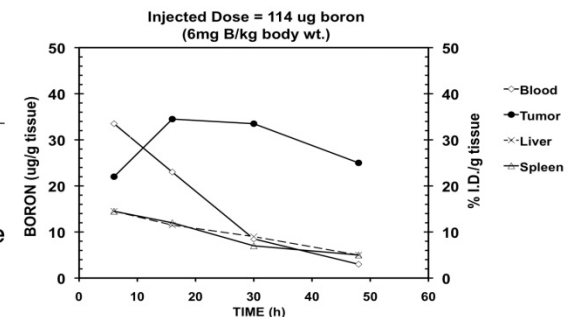
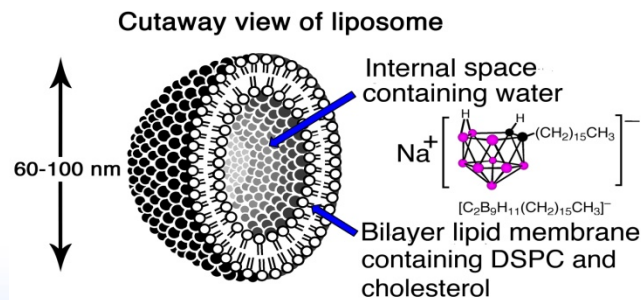
Conclusions/Path Forward

- **Neutronic performance of the new MURR thermal beamline is in the expected range**
- **We are proceeding with completion of thermal beamline shielding, interlocks, instrumentation, detailed spectral characterization and dosimetry**
- **Long-Term Collaborative Research Program:**



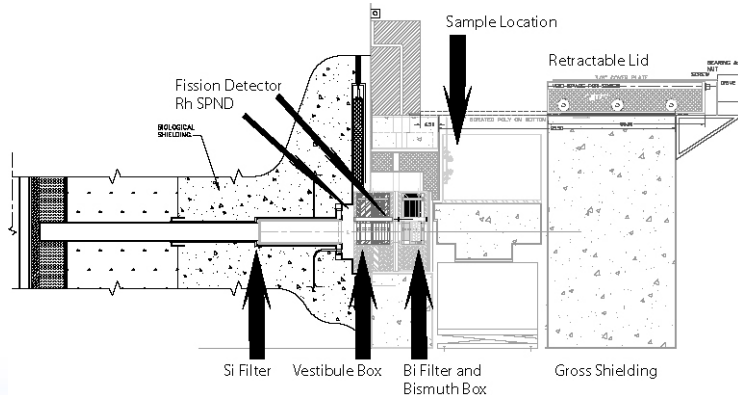
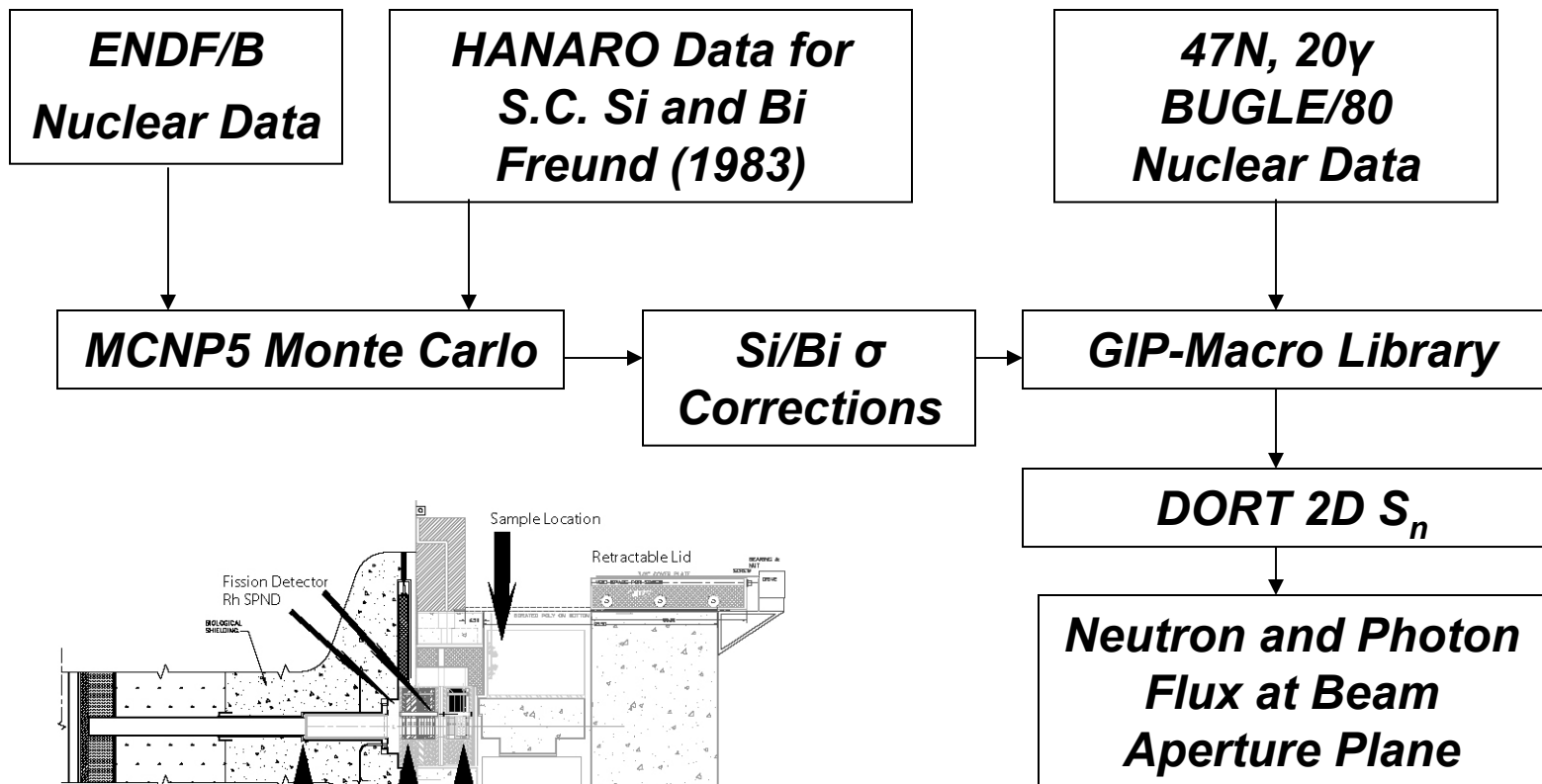
- **Small-animal studies at MURR using thermal beam (Advanced B_{10} and B_{20} Compounds, liposome encapsulation). Independent confirmation in collaboration with CNEA. Complementary large-animal studies at Washington State University epithermal facility.**

- **Installation of epithermal beam and conduct of large-animal studies and, ultimately, human trials at MURR**

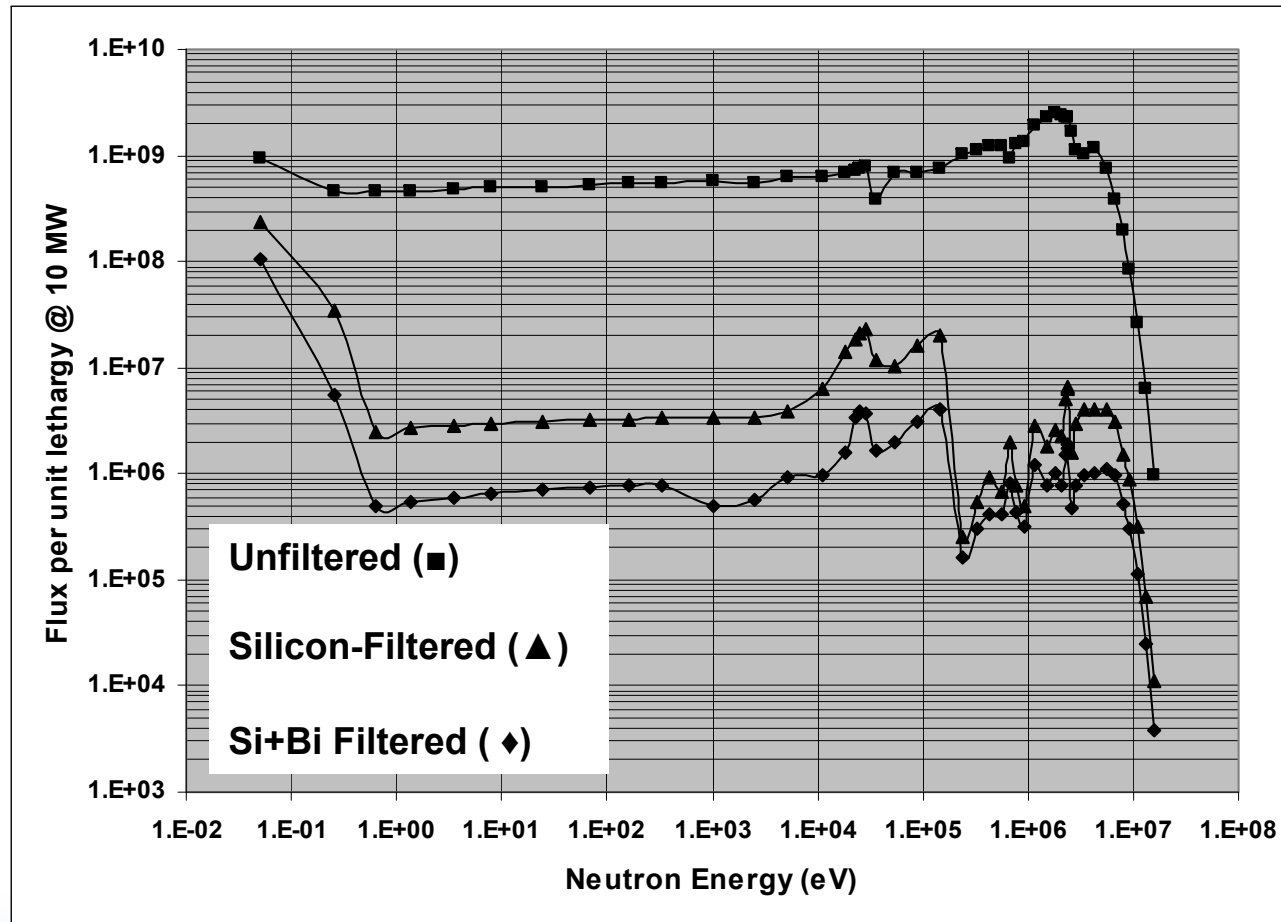


Backup Information

Original Computational Modeling



Unfiltered and Filtered MURR Beamline E Spectra – Discrete-Ordinates Simulation (DORT)



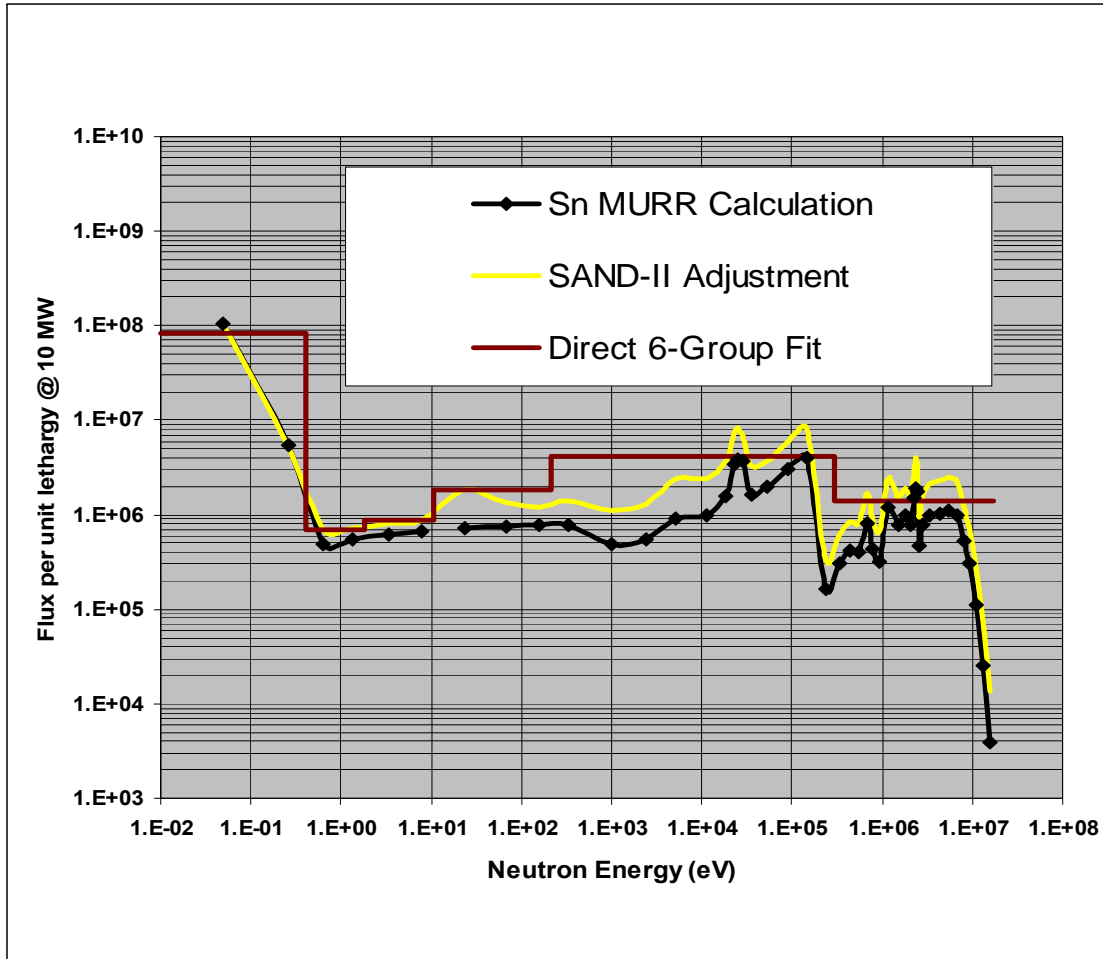
Configuration for Initial Crystal Thickness Scoping Studies



Preliminary Neutronic Performance Results for the Thermal Neutron NCT Research Facility at MURR

	<u>Voided Beamline</u>	<u>8 cm Bi Crystal</u>	<u>50 cm Si Crystal</u>	<u>50 cm Si + 8 cm Bi</u>
Saturation Activity, Bare Gold Foil (Bq/atom)	1.31×10^{-12} (5%)	3.82×10^{-13} (5%)	2.38×10^{-13} (5%)	8.67×10^{-14} (5%)
Saturation Activity , Cd Gold Foil (Bq/atom)	4.11×10^{-13} (5%)	7.49×10^{-14} (5%)	3.64×10^{-15} (5%)	8.21×10^{-16} (5%)
Difference in Saturation Activity (Bq/atom)	8.95×10^{-13} (8%)	3.07×10^{-13} (5%)	2.34×10^{-13} (5%)	8.59×10^{-14} (5%)
Measured Thermal Flux (n/cm²-s)	9.80×10^9 (11%)	3.36×10^9 (8%)	2.56×10^9 (8%)	9.40×10^8 (8%)
Calculated Thermal Flux from DORT (n/cm²-s)	9.38×10^9 (10%)	3.81×10^9 (10%)	2.22×10^9 (10%)	9.62×10^8 (10%)
Cadmium Ratio	3.18 (7%)	5.10 (7%)	65.3 (7%)	105.5 (7%)
Wire saturation activity ratio (Au/Cu)	36.4	28.4	22.4	22.4

Initial Neutron Spectrum Measurement Results– MURR Beamline E



Estimated Dosimetric Parameters

$$\Phi_{th} = 8.84 \times 10^8 \text{ n/cm}^2\text{-s} (\pm 5.5\%)$$

$$D_H = 1.37 \text{ cGy/min}$$

$$K_H = 2.57 \times 10^{-11} \text{ cGy-cm}^2$$

$$D_N = 1.14 \text{ cGy/min}$$

$$K_N = 2.15 \times 10^{-11} \text{ cGy-cm}^2$$

$$D_B = 0.43 \text{ cGy/m/ppm B}$$

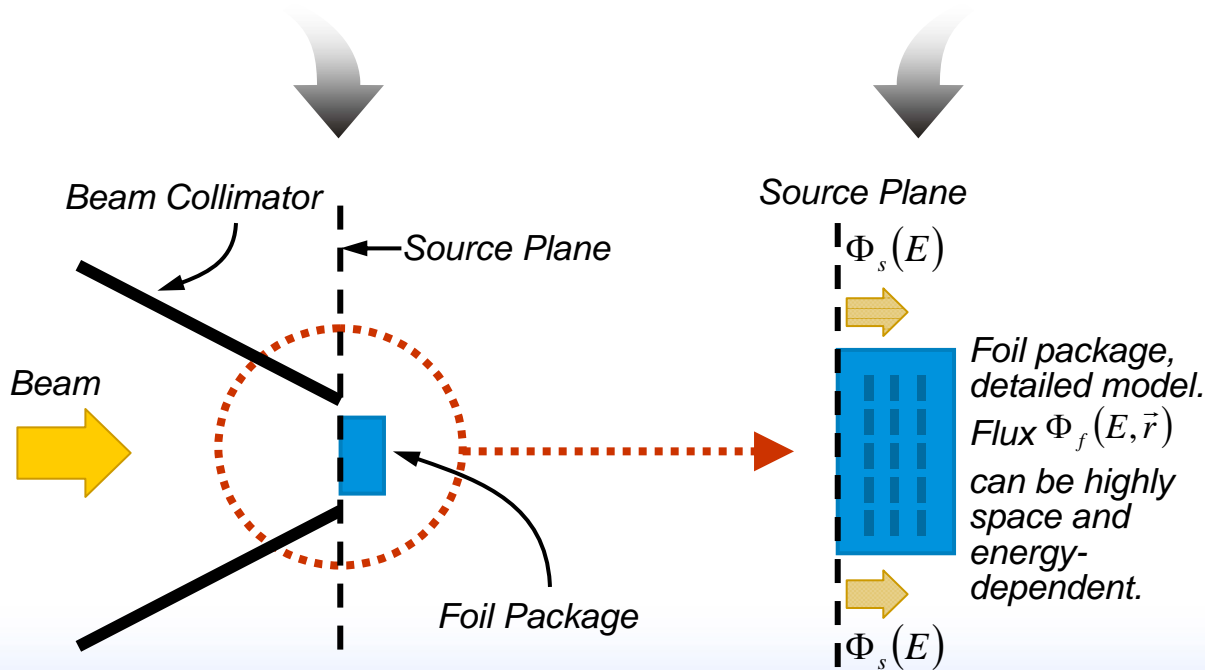
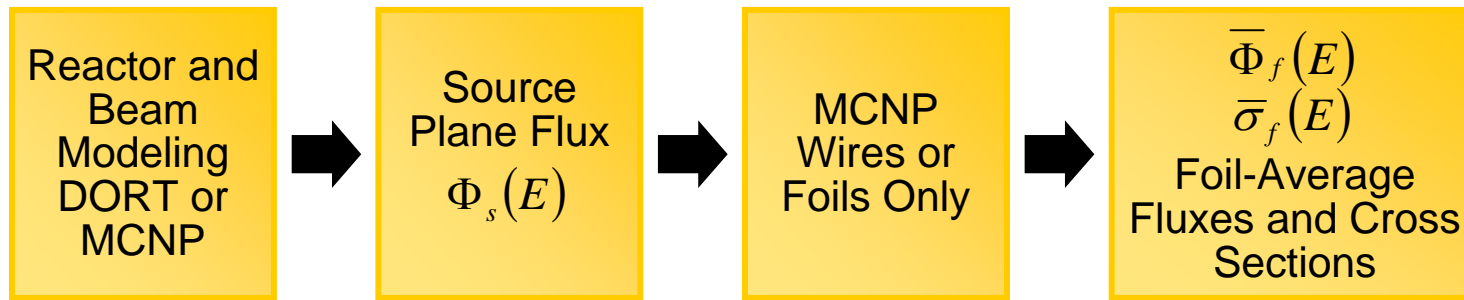
$$D_\gamma = 2.12 \text{ cGy/min (calculated)}$$

Spectral Fit Parameters:

$$\text{Reduced } X^2 = 0.29 \text{ (Direct)}$$

$$\text{Reduced } X^2 = 0.99 \text{ (SAND-II)}$$

Computation of Unfolding Parameters – General Case



$$\bar{\Phi}_f(E) = \frac{\int_{V_f} \Phi_f(E, \vec{r}) dV}{V_f}$$

$$\bar{\sigma}_f(E) = \frac{\int_{V_f} \sigma_f(E) \Phi_f(E, \vec{r}) dV}{\int_{V_f} \Phi_f(E, \vec{r}) dV}$$

$$\int_0^{\infty} \bar{\sigma}(E) \cdot \bar{\Phi}_f(E) dE = \text{Reaction Rate}$$

Method for Direct Unfolding of Neutron Spectra

The volume-average activation rate per atom for a foil dosimeter placed in a neutron flux field may be calculated as:

$$R = \int_0^{\infty} \sigma_f(E) \Psi_f(E) dE \quad (1)$$

where $\sigma_f(E)$ is the microscopic activation cross section of interest for the foil material, as a function of neutron energy and $\Psi_f(E)$ is the volume-average scalar neutron flux within the foil, again as a function of energy. Equation 1 can also be expressed as:

$$R = \int_0^{\infty} \sigma_f(E) \left(\frac{\Psi_f(E)}{\Psi(E)} \right) \Psi(E) dE = \int_0^{\infty} \sigma_f(E) P_f(E) \Psi(E) dE \quad (2)$$

where $\Psi(E)$ is the unperturbed neutron flux that would exist at the measurement location in the absence of the foil and any surrounding spectral modification devices (Cd covers, boron sphere, etc).

Equation 2 may be written as a summation rather than as an integral by partitioning the range of the energy variable into a number of discrete contiguous energy groups:

$$R = \sum_{j=1}^{NG} a_j \phi_j \quad (3)$$

where NG is the total number of energy groups,

$$a_j = \frac{\int_{EL_j}^{EH_j} \sigma_f(E) P_f(E) \Psi(E) dE}{\int_{EL_j}^{EH_j} \Psi(E) dE} \quad (4)$$

and

$$\phi_j = \int_{EL_j}^{EH_j} \Psi(E) dE. \quad (5)$$

where EL_j and EH_j are the lower and upper energy limits of energy group j .

If additional foils are placed in the beam, or if a particular foil exhibits more than one activation response then Equation 3 may be written as a system of equations:

$$R_i = \sum_{j=1}^{NG} a_{ij} \phi_j \quad (6)$$

where R_i is the total activation rate for interaction i and a_{ij} is the activation constant from Equation 4 for reaction i due to neutrons in energy group j . There will be a total of NF equations, where NF is the total number of activation responses available.

In practical applications the functions $\sigma_f(E)$, $P_f(E)$, and $\Psi(E)$ are ordinarily not continuous functions. The INL has adopted a standard using 47-group representations of the actual functions, discretized according to the BUGLE-80 neutron energy structure. The integrals in Equations 4 and 5 are therefore actually summations over the fine-group structure within each broad group used for spectral unfolding.

The system of activation equations, Eq. 6, may be written out in matrix form as:

$$\begin{bmatrix} a_{11} & a_{12} & a_{13} & \cdots & a_{1NG} \\ a_{21} & a_{22} & a_{23} & \cdots & a_{2NG} \\ a_{31} & a_{32} & a_{33} & \cdots & a_{3NG} \\ \vdots & \vdots & \vdots & & \vdots \\ \vdots & \vdots & \vdots & & \vdots \\ a_{NF1} & a_{NF2} & a_{NF3} & & a_{NF\ NG} \end{bmatrix} \begin{bmatrix} \phi_1 \\ \phi_2 \\ \phi_3 \\ \vdots \\ \phi_{NG} \end{bmatrix} = \begin{bmatrix} R_1 \\ R_2 \\ R_3 \\ \vdots \\ R_{NF} \end{bmatrix} \quad (7)$$

or, more compactly:

$$[A][\Phi] = [R] \quad (8)$$

When $NF > NG$ an approximation for the flux vector is sought such that the sum of the squares of the weighted differences between the measured reaction rates and the calculated reaction rates obtained by substituting the desired approximate solution vector into each row of Equation 7 is minimized. That is, we wish to minimize the quantity Δ ,

$$\Delta = \sum_{i=1}^{NF} \frac{\delta_i^2}{u_i^2} \quad (9)$$

where u_i is the experimental uncertainty associated with reaction rate i and

$$\delta_i = (R_i - (a_{i1}\phi + a_{i2}\phi_2 \cdots + a_{iNG}\phi_{NG})) \quad (10)$$

To accomplish this, Equation 10 is differentiated successively with respect to each group flux and the result in each case is set to zero. This produces a set of NG equations, one for each differentiation operation. Upon some additional manipulation the equations have the following compact form:

$$[A]^T [V] [A] [\Phi] = [A]^T [V] [R] \quad (11)$$

where $[V]$ is an $NF \times NF$ diagonal matrix whose elements are the inverse squares of the measurement uncertainties for the NF reaction rates:

i.e.

$$[V] = \begin{bmatrix} \frac{1}{u_1^2} & & & & 0 \\ & \frac{1}{u_2^2} & & & \\ & & \frac{1}{u_3^2} & & \\ & & & \dots & \\ 0 & & & & \frac{1}{u_4^2} \end{bmatrix} \quad (12)$$

Equation 11 can be expressed more compactly as:

$$[B][\Phi] = [S] \quad (13)$$

where the new matrix $[B] = [A]^T [V][A]$ will be of dimension $NG \times NG$ and the new vector $[S]$ will be of length NG . Equation 13 is then solved to yield the desired flux vector.

Propagation of uncertainties in the unfolding process can be analyzed using a standard approach. In general the measured reaction rates in Equation 11 will each have an associated experimental uncertainty. In addition there will be a component of variance in the unfolded fluxes associated with the nature of the least-squares process itself

An estimate for the variance of the unfolded flux in group j may be expressed as:

$$s_j^2 = \sum_{i=1}^{NF} \left(\frac{\partial \phi_j}{\partial R_i} \right)^2 [\delta_i^2 + u_i^2] \quad (14)$$

where δ_i is computed from Equation 10 and u_i is the experimental uncertainty associated with reaction rate i . To obtain the required matrix of derivatives the rows of Equation 11 are differentiated successively with respect to each reaction rate and the results are rearranged and combined to yield:

$$[B] \frac{\partial [\Phi]}{\partial R_i} = [\text{column } i \text{ of } [A]^T [V]] \quad (15)$$

Equation 15 describes NF systems of NG simultaneous equations that can be solved to obtain all of the derivatives necessary to evaluate Equation 14 for the uncertainties associated with the group fluxes.